Available online at www.sciencedirect.com
ScienceDirect
Polymer 48 (2007) 3593–3600
polymer
www.elsevier.com/locate/polymer

Free energy barrier for compact chains escaping from a small sphere

Yu Shen [a], Linxi Zhang [b,*]

[a] *Department of Physics, Zhejiang University, Hangzhou 310027, PR China*
[b] *Department of Physics, Wenzhou University, Wenzhou 325027, PR China*

Received 28 September 2006; received in revised form 18 April 2007; accepted 24 April 2007

Abstract

In this paper, the process of compact polymer chains escaping from a small sphere to a large one in the view of thermodynamics is investigated in detail based on the pruned-enriched-Rosenbluth method (PERM), which is quite efficient for the three-dimensional polymers on the simple-cubic lattice. In our simulation, three representative states of a polymer chain during the escaping process are studied, and some statistical properties of the chain size and the chain shape, such as mean-square radius of gyration per bond $\langle S^2\rangle/N$ and the shape factor $\langle\delta^*\rangle$ are investigated. Our aim is to illuminate how the size and shape of the compact chains change during the escaping process. The changes of $\langle S^2\rangle/N$ and $\langle\delta^*\rangle$ are not monotone and it is due to the fact that the chain should stretch itself in the escaping process. In the meantime, some thermodynamic properties are also calculated here. The hole is designed to be small enough to allow only one monomer at a time and it thus reduces the number of allowed chain conformations and breaks contacts between monomers at the beginning of the process. Additionally, we discuss the free energy barrier per bond $H_2 - H_1 = \Delta H$ of a compact chain, and here H_2 is the maximum free energy per bond during the process and H_1 is the minimum one when the compact chain is within the small sphere. Averaging free energy barrier over chain length N is convenient for the comparison with different chain lengths. ΔH as a function of chain length N and radius r_1 of the small sphere is also studied and our result shows that ΔH for longer chains is lower means that it is relatively easier for each bond in longer chains to surmount the free energy barrier to escape. Some discussions about the self-avoiding walk (SAW) and swollen chains are also made for the comparison, and our results also show that the restriction of the small sphere on the SAW and the swollen chains is more effective because of their relatively looser intrinsic structure.

Keywords: Free energy barrier; PERM; Translocation of compact chain

---

1. Introduction

Transport of molecules across membranes (such as cellular membrane) plays an important role for many biological processes. These molecules are often long, and the narrow pores in the membranes do not allow them to pass through as a single unit. They have to thus squeeze – i.e., translocate – themselves through the pores. DNA, RNA, and proteins are such naturally occurring long molecules [1–3] in a variety of biological processes. Translocation is also used in gene therapy [4] and in delivery of drug molecules to their activation sites [5,6]. In addition to its biological relevance, the translocation dynamics is also a challenging topic in polymer physics. Accordingly, the polymer translocation has attracted a considerable number of experimental [7–14] and theoretical [15–33] studies.

The translocation of a polymer through a nanopore faces a large entropic barrier due to the loss of a great number of available configurations. In order to overcome the barrier and to speed up the translocation, an external field or interaction is often introduced. The possible driving mechanisms include an external electric field, a chemical-potential difference, or selective adsorption on one side of the membrane. For example, in 1996, Kasianowicz et al. [7] reported that an electric field can drive single-strand DNA and RNA molecules through the α-hemolysin channel with an inside diameter of 2 nm and that the passage of each molecule is signaled by the blockade in the channel current.

---

* Corresponding author.
E-mail address: lxzhang@hzcnc.com (L. Zhang).

0032-3861/$ - see front matter © 2007 Published by Elsevier Ltd.
doi:10.1016/j.polymer.2007.04.052

Inspired by the experiments, a number of recent theories [15–33] have been developed for the behaviors of polymer translocation. Even without an external driving force, polymer translocation remains a challenging problem. Although the actual system is complicated by many biological factors, many scientists are trying to use simple model to explore the process of translocation. Sung and Park [16] have studied the transport of a Gaussian chain under the special conditions where the segment friction across the pore is proportional to the polymer length. Recent simulation studies [31,32] have shown that it is possible to capture many essential features of the translocation process using an appropriate one-dimensional model. Di Marzio and Mandell [18,33] have investigated the equilibrium properties of a polymer molecule whose two ends reside on opposite sides of a membrane or partition separating two solutions in the limit of no self excluded volume. Muthukumar [30] has treated the process with classical nucleation theory in which the monomer friction is taken to be dictated by the ratchet potential associated with the pore and free energy barrier for polymer chains escaping from a small sphere (similar to cell) was qualitatively predicted. In his another work, free energy barrier and mean translocation time are studied for the movement of a single Gaussian chain and a self-avoiding one from one sphere to another one through a narrow pore using the self-consistent field theory formalism [20,21]. The free energy landscape for polymer translocation is significantly modified by excluded volume interactions among monomers. Free energy barrier is such a familiar phenomenon that Hu et al. [34,35] has also reported free energy barrier to melting of single-chain polymer crystallite. Also, free energy barrier appears in our simulation. In this paper, using PER method, we not only further validate the Muthukumar's result in Ref. [30] and discuss in detail the free energy barrier for different kinds of chains with different chain lengths N and different geometrical conditions, but also give some other quantitative and comparative results, such as the chain size and the chain shape, during the process of translocation.

2. Simulation method

We study the escaping behaviors of compact chains, self-avoiding walk (SAW) chains and swollen chains from a small sphere (donor) to another large sphere (recipient) according to the model of a self-avoiding chain with chain length N on square lattice. Here we only take into account the contact interactions between monomers in order to analyze the different behaviors for compact chains, SAW chains, and swollen chains. The Hamiltonian of the system can be defined as:

$$E = \sum_{i<j} \varepsilon_{ij} \Delta(r_i - r_j) \qquad (1)$$

where ε_{ij} is the contact energy between monomer i and j, and $\Delta(r_i - r_j) = 1$ if r_i and r_j are adjoining lattice sites with i and j not adjacent along the chain, while $\Delta(r_i - r_j) = 0$ otherwise. $\varepsilon_{ij} = \varepsilon$ is assumed to -1 (compact chain), 0 (SAW chain) and 1 (swollen chain) (in the unit of $k_B T$) [36]. The compact conformations of polymers are important because they are the principal configurations of the native states of globular proteins [36]. Here a simple-cubic lattice is adopted, and the bond connecting adjacent monomers is fixed to a length of lattice constant, so the bond potential needn't be considered.

A new and effective simulation method is used here, which is called the pruned-enriched-Rosenbluth method (PERM) [37,38]. Grassberger has used this algorithm for simulating flexible chain polymers and their results can illuminate that this method is the most efficient for three-dimensional polymers on the simple-cubic lattice. Also PERM can be used to calculate the partition function instead of the enumeration calculation method. PERM has been extensively adopted in some simulations [39–42]. For example, Hsu and Grassberger studied a single flexible chain grafted to a membrane which has pores of size slightly larger than the monomer size using PERM [41,42]. In fact, the energy calculation in our simulation is similar in essence to that in these works. We also compare the partition function for two-dimensional 28-bond compact chains using the enumeration calculation method with the partition function using PERM, and find that the difference is only 1.2%. Therefore, we think that the PERM can be adopted in our calculation, and the results are reliable.

In Fig. 1, schematics are drawn to describe the whole process of a polymer chain escaping from the donor sphere (the small sphere) to the recipient one (the large sphere). The radius of the small sphere (the donor sphere) is r_1, and the radius of the large sphere (the recipient sphere) is r_2, which sets to a fixed value of 20 in this paper. Three representative states of the polymer chain during the process are noted as I, II, and III separately, and the detailed information can be seen in Fig. 1. In our model, we focus our attention on state II and compare it with states I and III. We use the percentage of the bonds of the chain locating in the small sphere (N_1/N) to characterize the process of escaping from the small sphere. With the decrease of $p = N_1/N$, the polymer chain gradually escapes from the small sphere and enters into the large one. We count the total conformations in different states (with different N_1/N), and our aim is to investigate how the compact chains, the SAW chains, and the swollen chains escape from the small sphere to the large sphere, how the height of free energy barrier depends on N and r_1, and how the chain size and energy change in the escaping process.

The partition function of the system is

$$Z = \sum_i \exp(-E_i/k_B T) \qquad (2)$$

where $\sum_i$ is the sum of all conformations.

The average Helmholtz free energy of the polymer chains can be derived from the partition function:

$$A = -k_B T \ln Z \qquad (3)$$

This parameter can supply much important thermodynamic information for chains [43–46].

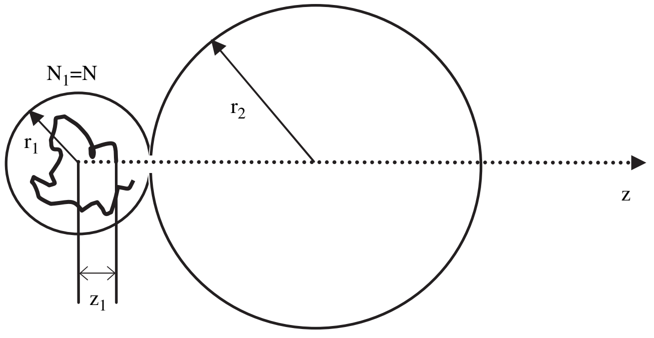

(a) State I

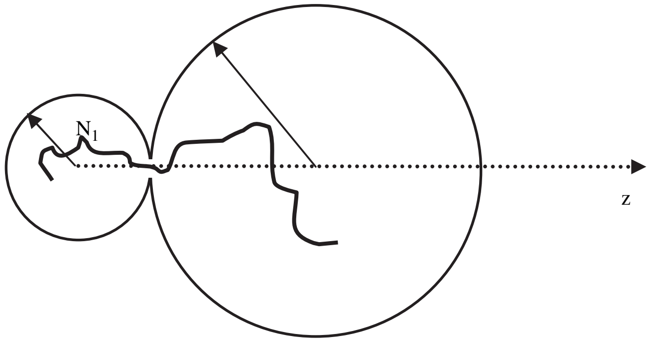

(b) State II

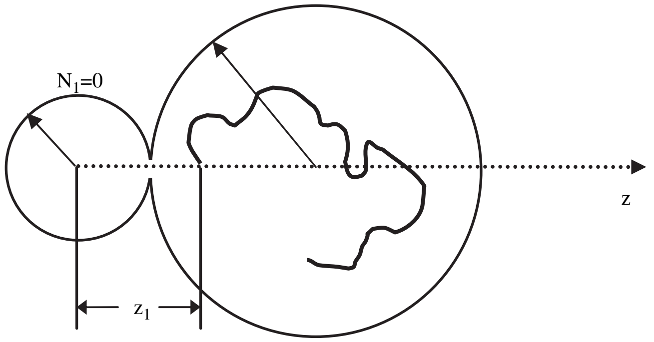

(c) State III

Fig. 1. Three representative conformations during the process of escaping from a small sphere. Here the radii of the small and the large sphere are r_1 and r_2, respectively, and r_2 is set to a fixed value of 20. (a) The chain is within the small sphere completely with $z_1 < r_1$ and $N_1 = N$; (b) part of the chain (N_1) is within the small sphere, while the other ($N - N_1$) is within the large one. The ratio of $p = N_1/N$ decreases little by little during the escaping process; (c) the chain has escaped completely from the small sphere with $z_1 > r_1$ and $N_1 = 0$.

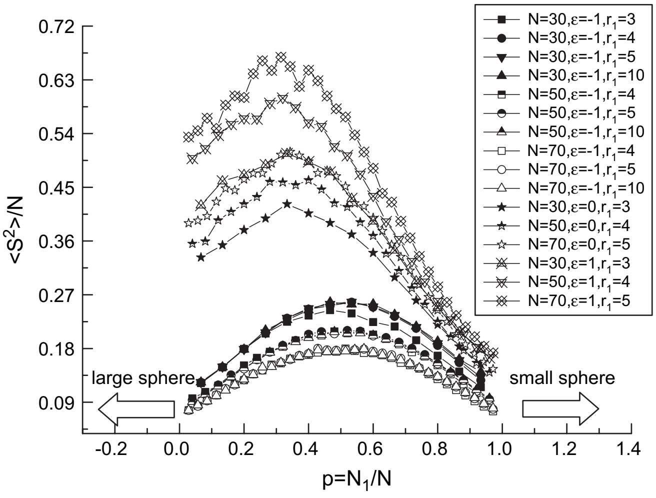

Fig. 2. Mean-square radius of gyration per bond $\langle S^2 \rangle/N$ vs. $p = N_1/N$ for compact chains ($\varepsilon = -1$), SAW chains ($\varepsilon = 0$) and swollen chains ($\varepsilon = 1$) in the process of escaping from the small sphere. $p = 1.0$ (i.e., $N_1 = N$) means that the whole chain is within the small sphere, while $p = 0$ (i.e., $N_1 = 0$) means that the whole chain has escaped completely from the small sphere.

3. Results and discussion

3.1. Chain size and shape

The mean-square radius of gyration per bond $\langle S^2 \rangle/N$ is plotted vs. p for compact polymer chains and SAW polymer chains in Fig. 2. The abscissa of the figure is the percentage of bonds of the chain located in the small sphere, which is defined as

$$p = N_1/N \tag{4}$$

where N_1 represents the number of bonds located in the small sphere and N is the chain length. Here $p = 1.0$ ($N_1 = N$) means that the whole chain is within the small sphere, while $p = 0$ ($N_1 = 0$) means that the chains have escaped completely from the small sphere. Now we pay our attention on the escaping process with p decreasing little by little (see state II). During the process of escaping from the small sphere to the large one, namely with p decreasing, the mean-square radii of gyration $\langle S^2 \rangle/N$ for compact chains and SAW chains with different chain lengths N all increases first and then decreases. There exists a peak in each curve. The peaks for SAW chains ($\varepsilon = 0$) and swollen chains ($\varepsilon = 1$) locate at smaller value of p than that for compact chains ($\varepsilon = -1$), and the influence of contact interactions between monomers on the variation range of the chain size is obvious during the escaping process. On the whole, values of $\langle S^2 \rangle/N$ for SAW and swollen chains are obviously larger than that for compact chains. With gradually entering into the larger sphere, swollen chains with $\varepsilon = 1$ grow larger in size than SAW chains with $\varepsilon = 0$ because of the stronger excluded volume interaction for $\varepsilon = 1$. For SAW or swollen chains, the longer the chain is, the larger the value of $\langle S^2 \rangle/N$ is. For compact chains, however, the values of $\langle S^2 \rangle/N$ increase with the decrease of chain length N, which indicates that for longer compact chain, the effects of contact interactions are more obvious. It is noticeable that in the case of $r_1 = 3$, $\langle S^2 \rangle/N$ is obviously smaller than that in the other cases because of the stronger and more effective restriction for $r_1 = 3$. When $\varepsilon = 0$ and $\varepsilon = 1$, the value of $\langle S^2 \rangle/N$ at small p is much larger than that at large p, and when $\varepsilon = -1$, the difference in the value of $\langle S^2 \rangle/N$ between two sides of the peak is not large, reflecting that the restriction of the small sphere on the SAW and the swollen chains is more effective.

In order to investigate the change in the shape of a polymer chain during the escaping process in more detail, we consider the radius of gyration tensor S, which is defined as:

$$S = \frac{1}{N+1}\sum_{i=0}^{N} S_i S_i^T = \begin{pmatrix} S_{xx} & S_{xy} & S_{xz} \\ S_{yx} & S_{yy} & S_{yz} \\ S_{zx} & S_{zy} & S_{zz} \end{pmatrix} \tag{5}$$

where $S_i = \mathrm{col}(x_i, y_i, z_i)$ is the position of monomer i in a frame of reference with its origin at the center of a chain. The tensor S can be diagonalized to form a diagonal matrix with three eigenvalues L_1^2, L_2^2, and L_3^2 $(L_1^2 \le L_2^2 \le L_3^2)$. Solc and Stockmayer first used the ratio of these parameters $\langle L_1^2 \rangle : \langle L_2^2 \rangle : \langle L_3^2 \rangle$ to measure the shape of a flexible polymer chain [47,48], and they estimated the ratio to be 1:2.7:11.7 based on a random walk of 100 bonds on a simple-cubic lattice using Monte Carlo (MC) technique. According to three eigenvalues from Eq. (5), another valuable parameter [49,50] for the shape of chains may be obtained by combining the reduced components to a single quantity that varies between 0 (sphere) and 1 (rod) is defined as:

$$\langle \delta^* \rangle = 1 - 3\left\langle \frac{L_1^2 L_2^2 + L_2^2 L_3^2 + L_1^2 L_3^2}{\left(L_1^2 + L_2^2 + L_3^2\right)^2} \right\rangle \tag{6}$$

$\langle \delta^* \rangle$ as a function of p for compact chains and SAW chains with different chain lengths N are shown in Fig. 3. For compact chains, the shape is spherical at the beginning of the process, and then the shape approaches clubbed because during the escaping process the chain should stretch itself, and at last it restores to be spherical shape again due to the contact interactions between monomers. The structure of SAW and swollen chains is inclined to be loose relatively, so with the decrease of p, $\langle \delta^* \rangle$ for SAW and swollen chains grows larger than that for compact chains, showing that the restriction of the small sphere on the chains with $\varepsilon = 0$ and $\varepsilon = 1$ is more effective. Otherwise, $\langle \delta^* \rangle$ for swollen chains is slightly larger than that for SAW chains when most of the bonds have entered into the larger sphere because the structure of the swollen chains is looser than that of the SAW chains. However, the trends of $\langle \delta^* \rangle$ for SAW and swollen chains are alike, and the curves with same ε almost overlap.

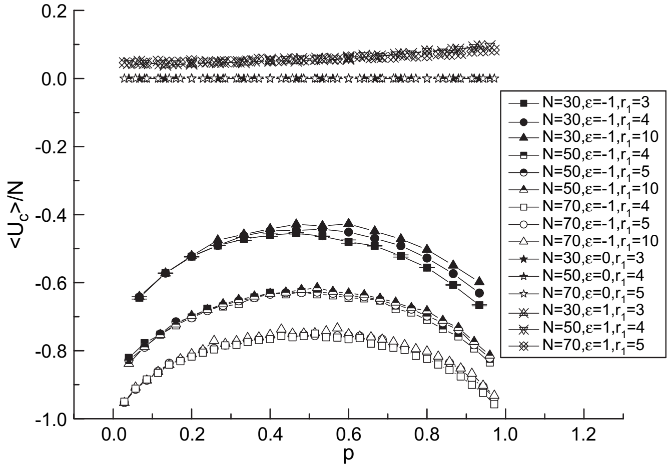

Fig. 4. Average contact energy per bond $\langle U_c \rangle / N$ vs. $p = N_1/N$ for compact chains ($\varepsilon = -1$), SAW chains ($\varepsilon = 0$) and swollen chains ($\varepsilon = 1$).

3.2. Thermodynamics properties

Average energy per bond $\langle U_c \rangle / N$ as a function of p for compact chains, SAW chains and swollen chains with different chain lengths N are shown in Fig. 4. The energy calculation in our simulation is similar in essence to that in the work presented in Refs. [41,42]. As we only take into account the contact interactions between monomers, average energy per bond $\langle U_c \rangle / N$ is equal to 0 for SAW chains, and greater than 0 for swollen chains. $\langle U_c \rangle / N$ drops slightly with p decreasing for the swollen chains, and this means that the escape is spontaneous. $\langle U_c \rangle / N$ for compact chains ($\varepsilon = -1$) increases first with the decrease of p, and then decreases. There exists a peak in each curve, which predicates the change of the number of

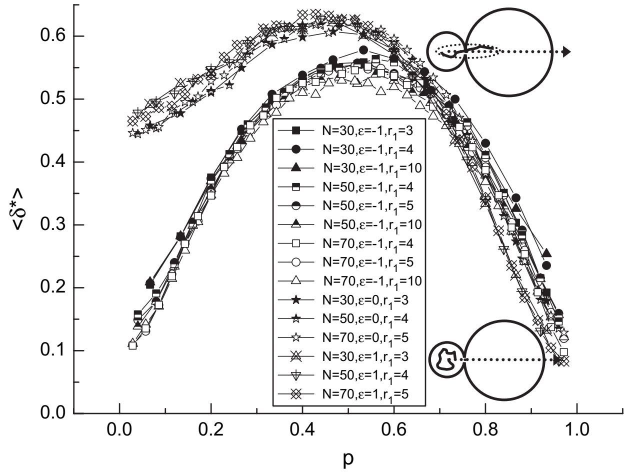

Fig. 3. Shape factor $\langle \delta^* \rangle$ vs. $p = N_1/N$ for compact chains ($\varepsilon = -1$), SAW chains ($\varepsilon = 0$) and swollen chains ($\varepsilon = 1$).

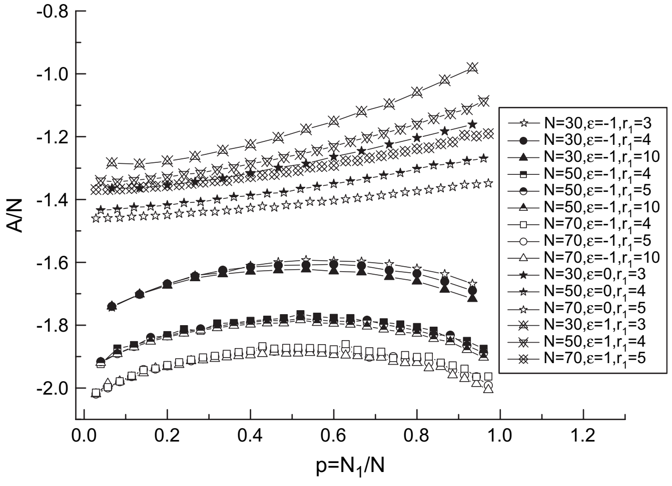

Fig. 5. Average free energy per bond A/N vs. $p = N_1/N$ for compact chains ($\varepsilon = -1$), SAW chains ($\varepsilon = 0$) and swollen chains ($\varepsilon = 1$).

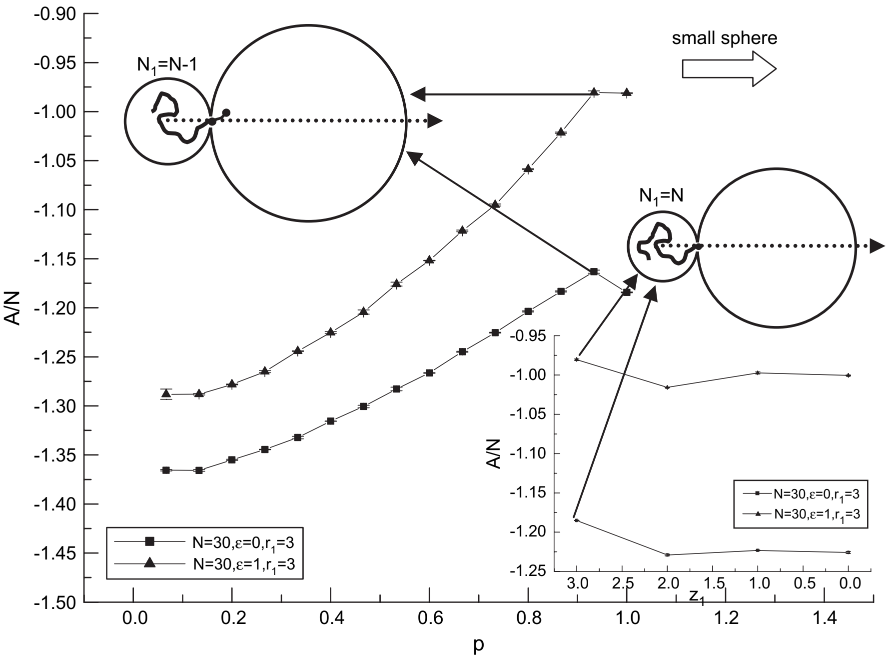

Fig. 6. Free energy per bond *A*/*N* for a 30-bond SAW ($\varepsilon = 0$) chain and a swollen one ($\varepsilon = 1$) with $r_1 = 3$ during the whole process including the case of the chain within the small sphere. The small inset denotes the changes of *A*/*N* within the small sphere with various positions of the first monomer. Here the error bars are also given in the figure.

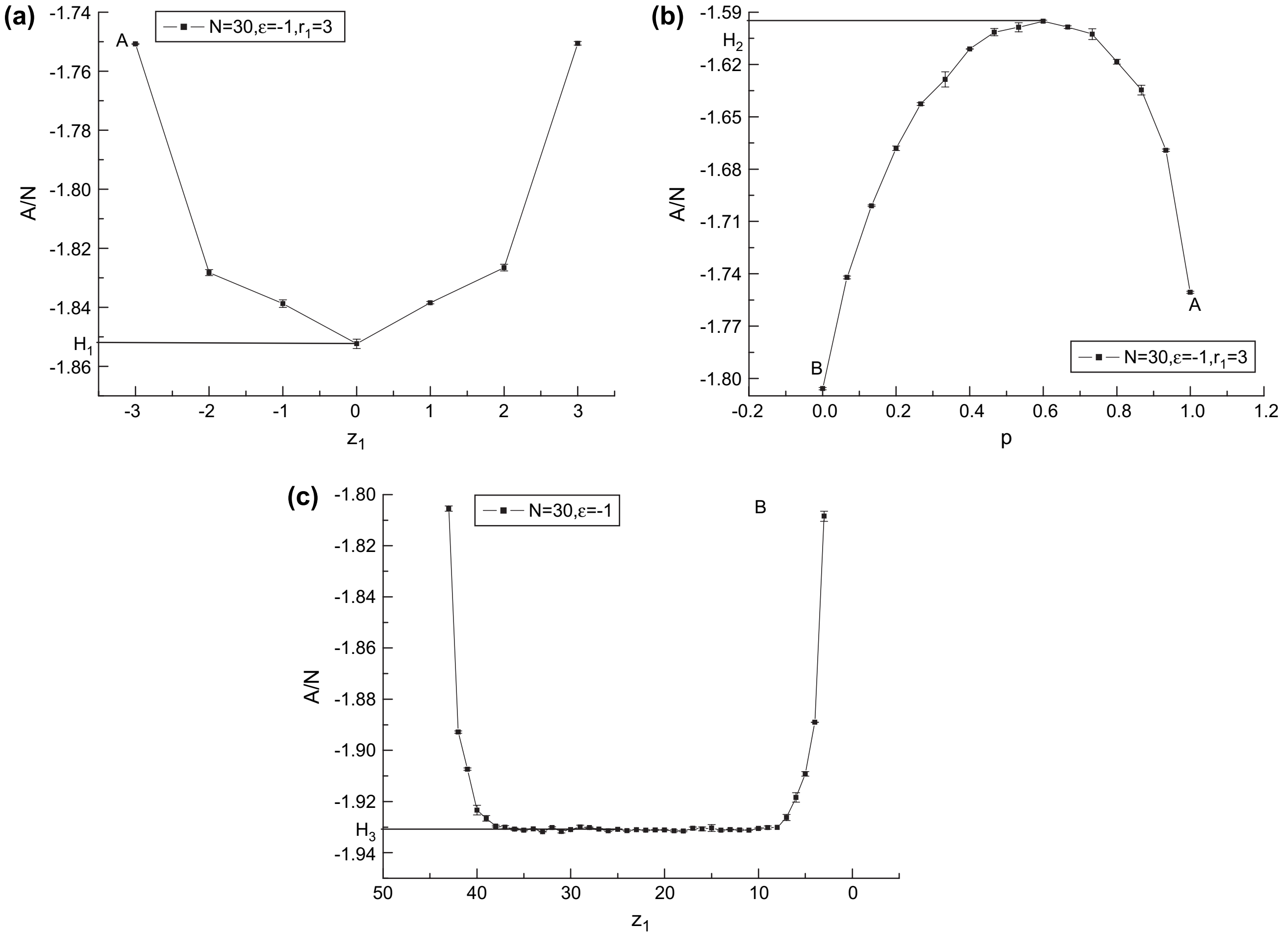

Fig. 7. Free energy per bond *A*/*N* for a 30-bond compact chain in different states during the whole process with $r_1 = 3$. (a) *A*/*N* as a function of z_1 (the *z*-coordinate of the first monomer) within the small sphere; (b) *A*/*N* vs. $p = N_1/N$ for the escaping process in state II; and (c) *A*/*N* as a function of $z_1(z_1 > r_1)$ in state III. Here H_1 represents the minimum average free energy within the small sphere, H_2 represents the maximum average free energy during the escaping process, and H_3 is the minimum average free energy within the large sphere ($H_3 < H_1$). Here the error bars are also given in the figure.

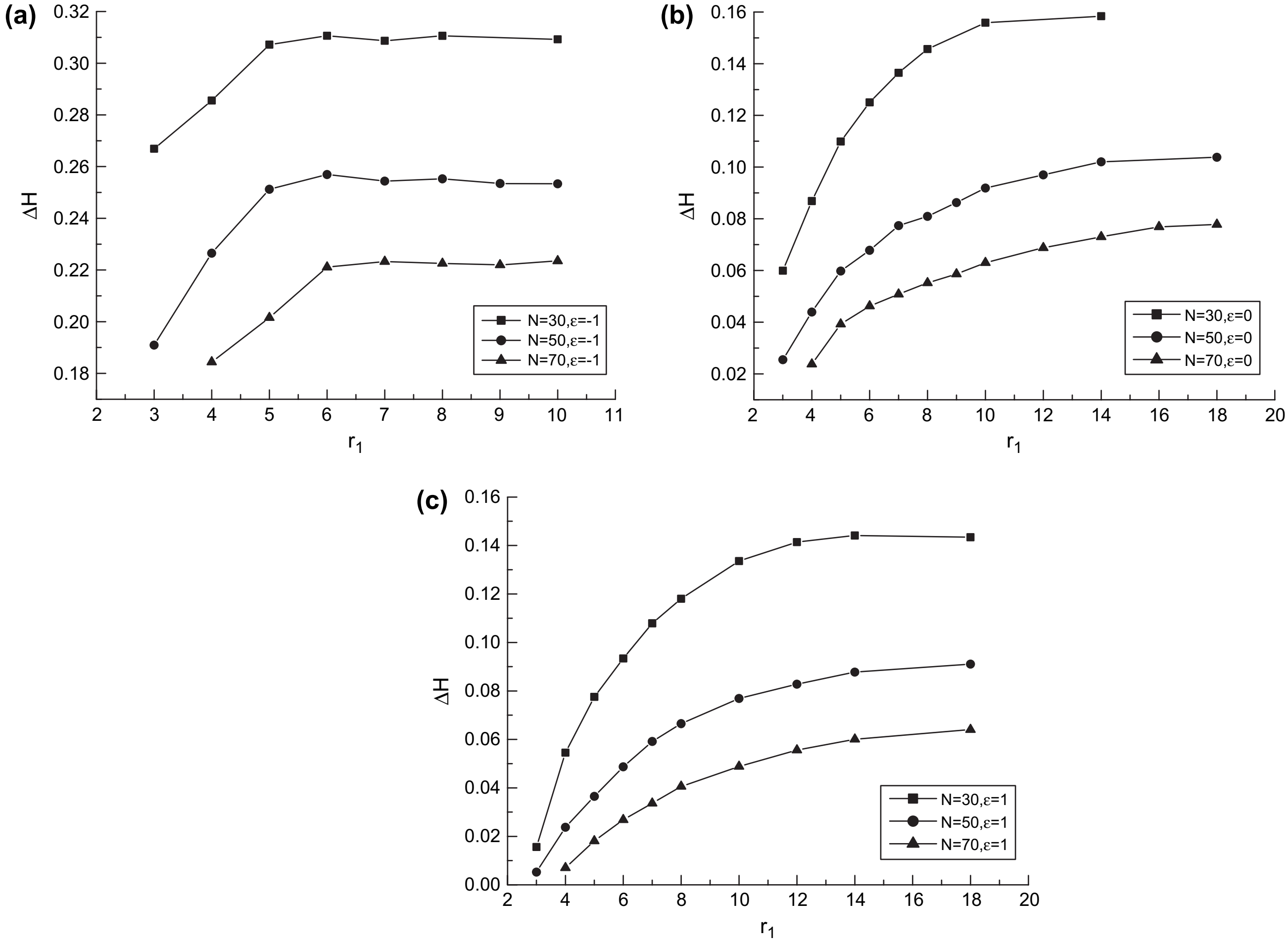

Fig. 8. Average free energy barrier per bond $\Delta H = H_2 - H_1$ vs. r_1 for (a) compact polymer chains, (b) SAW chains and (c) swollen chains. The definitions of H_1 and H_2 are given in Fig. 7.

contacts between monomers during the process. On the other hand, the value of $\langle U_c \rangle / N$ for compact chains increases with the decrease of chain length N, which is consistent with the results of $\langle S^2 \rangle / N$ in Fig. 2. Additionally, error bars are added to the curve with $N = 30$, $\varepsilon = -1$ and $r_1 = 3$ for example, and the errors are unconspicuous. This means that the PERM and the energy calculation are reasonable in our investigation of the translocation process.

Free energy per bonds A/N as a function of p for compact chains, SAW chains and swollen chains with different chain lengths are shown in Fig. 5. Similar to the case of $\langle U_c \rangle / N$, A/N for compact chains increases first with the decrease of p and then decreases, implying a free energy barrier in the escaping process. For SAW and swollen chains with small r_1, once one monomer has escaped from the small sphere, the process of escape is spontaneous, namely, the whole translocation of the chain in state II is spontaneous, which is essentially different from compact chains. A/N for swollen chains is larger than that for SAW chains, and A/N for SAW chains is larger than that for compact chains. Fig. 6 gives free energy per bond A/N for a 30-bond SAW chain and a swollen one with $r_1 = 3$ during the whole process and the small inset denotes the changes of A/N within the small sphere as a function of positions of the first monomer. In Ref. [21], the average free energy in the small sphere is calculated using the self-consistent field theory, and here the detailed change of the free energy with the different positions in the small sphere is discussed. For the SAW chain, a free energy barrier locates at $p \approx 0.9667$, and the chain should stretch itself to enter into state II. Once one monomer has escaped from the small sphere, the process of escape is spontaneous. In fact, a free energy barrier is an entropy barrier for SAW chains because of $A = U - TS \equiv -TS$. The behavior for swollen chains is the same as the SAW chains in essence. Errors of all data are given here, and they are quite small.

The free energy barrier for compact chains is also discussed here. We take 30-bond compact chains with $r_1 = 3$ for an example and the details can be seen in Fig. 7. Fig. 7 (a) represents A/N as a function of z_1 (the z-coordinate of the first monomer) for the compact chains within the small sphere, (b) represents A/N as a function of $p = N_1/N$ during the escaping process (state II), and (c) represents A/N as a function of $z_1 (z_1 > r_1)$within the large sphere (state III), in this case, the compact chains have escaped completely. There exists a barrier in each curve of free energy during the escape of compact chains from a small sphere to a larger one, and the reason may

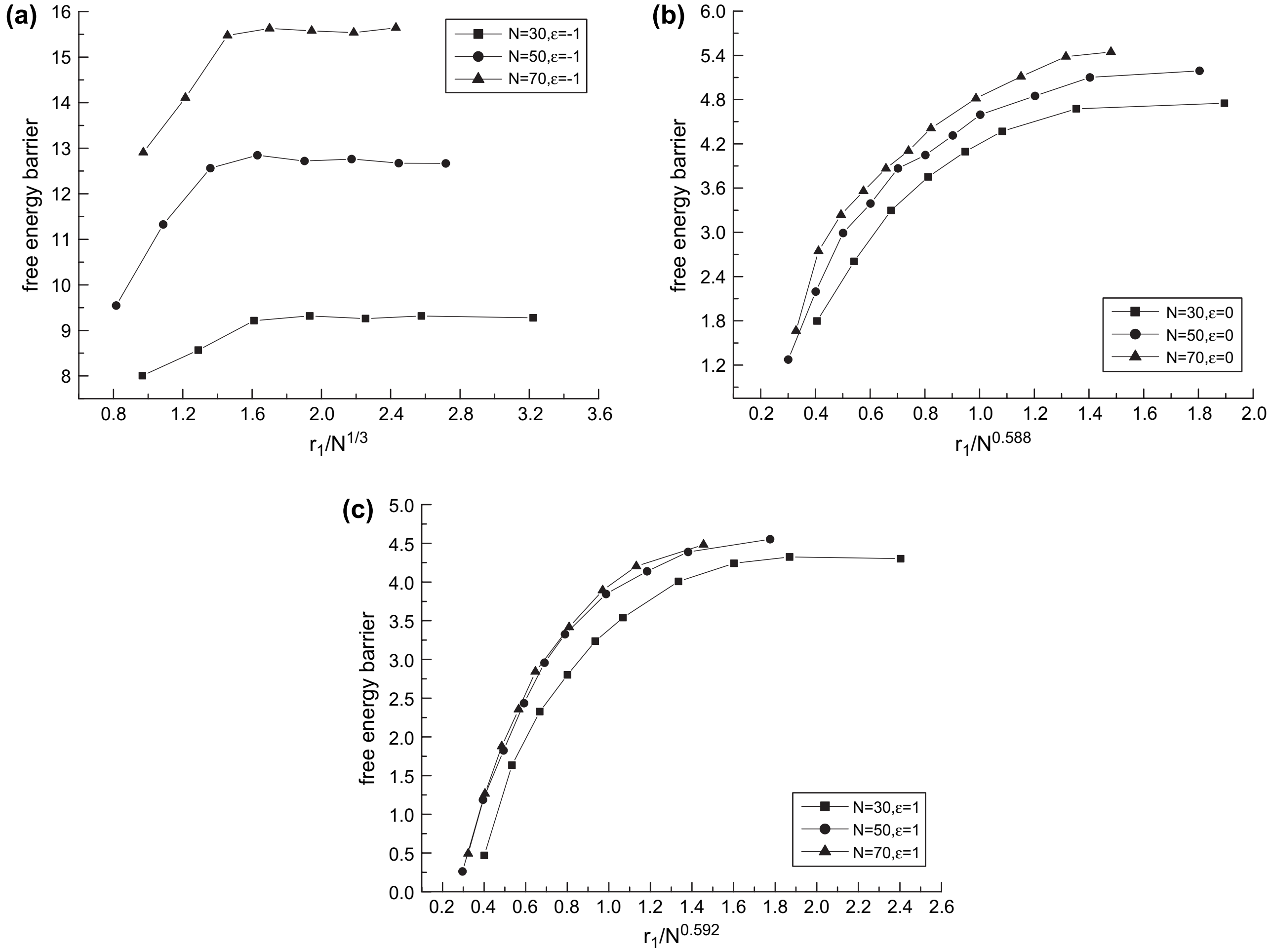

Fig. 9. Total free energy barrier vs. r_1/N^{γ} for (a) compact polymer chains, (b) SAW chains and (c) swollen chains. The size of the chain, such as the radius of gyration $\sqrt{\langle S^2 \rangle}$, scales as N^{γ}, and γ is equal to 1/3, 0.588 and 0.592 for compact, SAW and swollen chains, respectively [51,52].

be that in the process of escape the chain should be stretched. The minimum of A/N for compact chains in the initial state I (within the small sphere) is marked as H_1, and occurs when the first monomer of chains sits at the center of the small sphere, (see Fig. 7(a)). Similarly, we mark the maximum of A/N in state II as H_2, and the minimum of A/N in state III (in the large sphere) as H_3. Apparently, the value of H_3 is smaller than H_1, which is consistent with the fact presented in Ref. [30], and there exists a chemical-potential gradient $H_1 - H_3$ to push the polymer out of the small sphere. However, during the process from state I to state III, the chain must undergo the transition state illustrated in Fig. 1 (state II). Here the hole is designed to be small enough to allow only one monomer at a time, and this constraint reduces the number of allowed chain conformations and breaks contacts between monomers, therefore, this leads A/N to increase to H_2, and we define an average free energy barrier per bond as $H_2 - H_1 = \Delta H$.

Additionally, the dependence of ΔH on the radius r_1 of the small sphere for different chain lengths N is also discussed and the aim is to obtain more detailed information for the escaping process. The height of the barrier ΔH indicates the difficulty level of escape. In Fig. 8(a), ΔH increases with the increase of r_1 to a stable value separately for different chain lengths, which means that when the space of the small sphere increases to a certain degree enough for comfortable stay of the compact chain, the escape of the chain becomes more difficult. Our result that ΔH for longer chains is lower shows that it is relatively easier for each bond in longer chains to surmount the free energy barrier to escape. Fig. 8(b) and (c), respectively, shows the change of ΔH with r_1 for SAW chains and swollen chains. The values of ΔH are much smaller than that for compact chains, which indicates that the escape of SAW chains or swollen chains is much easier than that of compact chains. Values of ΔH for swollen chains are yet smaller than that for SAW chains. Besides, of SAW chains or swollen chains increases more slowly than that of compact chains when r_1 increases.

Fig. 9 shows the total free energy barrier for compact chains, SAW chains and swollen chains. For the purpose of making the restriction of the small sphere on the chains with different chain length equivalents, the abscissa of the figures is defined as r_1/N^{γ}, and γ is equal to 1/3, 0.588 and 0.592 for compact chains, SAW chains and swollen chains, respectively. The size of the chain, such as the radius of gyration $\sqrt{\langle S^2 \rangle}$, scales as N^{γ} [51,52]. In Fig. 9, the total free energy barrier is higher for larger N, especially for the compact chains, which is contrary to the case in Fig. 8. If the chain length is large enough, the total free energy barrier may be independent of the chain length for the SAW chains because the difference between the curves for 70-bond and 50-bond chains is much less than that for 50-bond and 30-bond chains. The case of the swollen chains is similar to that of the SAW chains, and the independent trend of the chain length for long chains is even more obvious. Comparing with compact chains SAW chains or swollen chains are more similar to DNA molecules.

4. Conclusion

In order to investigate the changes of chains in the size and shape during the escaping process, we first calculate the values of $\langle S^2\rangle/N$ and $\langle\delta^*\rangle$ for compact chains, SAW chains and swollen chains. Some thermodynamic properties are investigated as well. The most important information we obtain from our simulation is that there exists a free energy barrier $H_2 - H_1 = \Delta H$ during the escaping process. Moreover, our result that ΔH for longer chains is lower shows that it is relatively easier for each bond in longer chains to surmount the free energy barrier to escape. The values of free energy barrier for SAW chains or swollen chains are much smaller than that for compact chains, and the difference in free energy barrier for compact chains with different chain lengths is much larger than that for SAW chains or swollen chains. If the chain length is large enough, the total free energy barrier of the SAW chains or the swollen chains may be independent of the chain length.

Acknowledgments

This research was financially supported by National Natural Science Foundation of China (No. 20574052), Program for New Century Excellent Talents in Universities (NCET-05-0538) and Natural Science Foundation of Zhejiang Province (Nos. R404047 and Y405011). The authors thank the referees for their critical reading of the manuscript and their good ideas.

References

[1] Kaemmli UK, Favre M. J Mol Biol 1973;80:575–99.
[2] Alberts B, Bray D. Molecular biology of the cell. New York: Garland; 1994.
[3] Darnell J, Lodish H, Baltimore D. Molecular cell biology. New York: Scientific American Books; 1995.
[4] Szabò I, Bathori G, Tombola F, Brini M, Coppola A, Zoratti M. J Biol Chem 1997;272:25275–82.
[5] Tseng Y-L, Liu J-J, Hong R-L. Mol Pharmacol 2002;62:864–72.
[6] Tsutsui JM, Xie F, Porter RT. Cardiovasc Ultrasound 2004;2:23.
[7] Kasianowicz JJ, Brandin E, Branton D, Deaner DW. Proc Natl Acad Sci USA 1996;93:13770–3.
[8] Aktson M, Branton D, Kasianowicz JJ, Brandin E, Deaner DW. Biophys J 1999;77:3227–33.
[9] Meller A, Nivon L, Brandin E, Golovchenko JA, Branton D. Proc Natl Acad Sci USA 2000;97:1079–84.
[10] Henrickson SE, Misakian M, Robertson B, Kasianowicz JJ. Phys Rev Lett 2000;85:3057–60.
[11] Meller A, Nivon L, Branton D. Phys Rev Lett 2001;86:3435–8.
[12] Sauer-Budge AF, Nyamwanda JA, Lubensky DK, Branton D. Phys Rev Lett 2003;90:238101(1–4).
[13] Meller A. J Phys Condens Matter 2003;15:R581–607.
[14] Storm AJ, Storm C, Chen J, Zandbergen H, Joanny J-F, Dekker C. Nano Lett 2005;5:1193–7.
[15] Simon SM, Reskin CS, Oster GF. Proc Natl Acad Sci USA 1992;89:3770–4.
[16] Sung W, Park PJ. Phys Rev Lett 1996;77:783–6.
[17] Park PJ, Sung W. J Chem Phys 1998;108:3013–8.
[18] Di Marzio EA, Mandell AL. J Chem Phys 1997;107:5510–4.
[19] Muthukumar M. J Chem Phys 1999;111:10371–4.
[20] Muthukumar M. J Chem Phys 2003;118:5174–84.
[21] Muthukumar M. J Chem Phys 2004;120:3460–6.
[22] Lubensky DK, Nelson DR. Biophys J 1999;77:1824–38.
[23] Slonkina E, Kolomeisky AB. J Chem Phys 2003;118:7112–8.
[24] Chuang J, Kantor Y, Kardar M. Phys Rev E 2002;65:011802(1–8).
[25] Kantor Y, Kardar M. Phys Rev E 2004;69:021806(1–12).
[26] Ambjörnsson T, Apell SP, Konkoli Z, Di Marzio EA, Kasianowicz JJ. J Chem Phys 2002;117:4063–73.
[27] Gerland U, Bundschuh R, Hwa T. Phys Biol 2004;1:19–26.
[28] Baumgärtner A, Skolnick J. Phys Rev Lett 1995;74:2142–5.
[29] Wolterink JK, Barkema GT, Panja D. Phys Rev Lett 2006;96:208301.
[30] Muthukumar M. Phys Rev Lett 2001;86:3188–91.
[31] Chern S, Cardenas AE, Coalson RD. J Chem Phys 2001;115:7772–82.
[32] Tian P, Smith GD. J Chem Phys 2003;119:11475–83.
[33] Di Marzio EA, Kasianowicz JJ. J Chem Phys 2003;119:6378–87.
[34] Hu WB, Frenkel D, Mathot VBF. J Chem Phys 2003;118:3455–7.
[35] Hu WB, Frenkel D, Mathot VBF. arxiv:cond-mat/0206584.
[36] Chan HS, Dill KA. Macromolecules 1989;22:4559–73.
[37] Grassberger P. Phys Rev E 1997;56:3682–93.
[38] Combe N, Vlugt TJH, Wolde PRT, Frenkel D. Mol Phys 2003;101:1675–82.
[39] Zhang LX, Su JY. Polymer 2006;47:735–41.
[40] Zhang LX, Chen J. Polymer 2006;47:1732–40.
[41] Hsu H-P, Grassberger P. Europhys Lett 2007;77:18003(1–4).
[42] Hsu H-P, Paul W, Binder K. Europhys Lett 2006;76:526–32.
[43] Sun TT, Zhang LX, Chen J, Shen Y. J Chem Phys 2004;120:5469–75.
[44] Sun TT, Zhang LX, Su JY. J Chem Phys 2006;125:034702(1–8).
[45] Curro JG, Mark JE. J Chem Phys 1984;80:4521–5.
[46] Mark JE. J Phys Chem B 2003;107:903–13.
[47] Solc K, Stockmayer WH. J Chem Phys 1971;54:2756–7.
[48] Solc K. J Chem Phys 1971;55:335–44.
[49] Zifferer G, Preusser W. Macromol Theory Simul 2001;10:397–407.
[50] Jagodzinski O, Eisenriegler E, Kremer K. J Phys I 1992;2:2243–79.
[51] Kantor Y, Kardar M. Phys Rev E 1996;54:5263–7.
[52] Camacho CJ, Schanke T. Europhys Lett 1997;37:603–8.